

# Long-term Stable Field Electron Transfer from Carbon Nanotube Arrays at High Emission Current Densities

Jian-hua DENG, Zhao-xia PING, Rui-ting ZHENG and Guo-an CHENG\*

*Key Laboratory of Beam Technology and Material Modification of the Ministry of Education,  
College of Nuclear Science and Technology, Beijing Normal University, Beijing 100875, China*

(Received 30 December 2010)

The stability behaviors of multiwalled carbon nanotube arrays during field electron emission are studied. The results indicate that the stability, even at a high emission current density, has been greatly improved by an aging process, and a degradation of about 0.66% in the emission current density at  $21.86 \text{ mA/cm}^2$  during a 10-hour stability test has been obtained. A detailed analysis of the deterioration of the field electron emission characteristics is given, and the generation of Joule heat during field emission is found to be able to burn off the extruded carbon nanotubes, which will directly reduce the number of emission sites. On the other hand, the Joule heating effect may induce an annealing of the defects existing in the carbon nanotubes and may influence the distribution of electron energy states, both having a bad influence on the field emission characteristics. An aging process, especially aging at high emission current densities, can greatly reduce the influence of Joule-heating induced current degradation. Hence, an aging process at high emission current densities provides an effective way to realize long-term stable field electron emission from carbon nanotube arrays.

PACS numbers: 61.46.Np, 68.37.Vj, 79.70.+q

Keywords: Carbon nanotube arrays, Field emission, Stability, Aging process

DOI: 10.3938/jkps.58.897

## I. INTRODUCTION

Since the discovery of carbon nanotubes (CNTs) [1], due to their high aspect ratio, high mechanical strength, and superior electrical conductivity [2], they have proven to be an eminent material for field emitters, so, great efforts have been made to improve the growth process [3–5], the promotion of field electron emission characteristics [6–8], and so on. Long-term stable field electron emission is important for the realization of flat panel displays based on CNTs, and a great many works have been done to ameliorate the stability behaviors of field electron emission of carbon nanotube arrays (CNTAs). Zeng *et al.* reported that the emission current density of CNTAs only decreased 10% at about  $30 \text{ mA/cm}^2$  in 12 hours due to a thermal oxidation pretreatment, which was very good considering the large emission current density [9]. Reports from Chen *et al.* revealed that the emission current density showed no noticeable degradation at  $1 \text{ mA/cm}^2$  in 19 hours due to a tip sonication pretreatment that can effectively cut CNTs short and regulate the length of CNTs [10]. Hence, it's indispensable to find the very factors that will bring about a deterioration of the field emission (FE) characteristics and to try

to promote stability behavior in CNTAs.

In this research, stability measurements on CNTAs at different emission current densities were carried out. A detailed analysis of the degradation of the emission current density during the FE measurements is given, and an effective way to promote the stability behavior in CNTAs will be provided.

## II. EXPERIMENTS AND DISCUSSION

The CNTs were synthesized by using thermal chemical vapor deposition on an iron-ion pre-bombarded n-type (100) silicon substrate at  $750^\circ\text{C}$  and ambient pressure. During CNT growth, acetylene ( $\text{C}_2\text{H}_2$ ) and hydrogen ( $\text{H}_2$ ) with a flux rate of 87:600 were utilized as the carbon source and the carrying gas, respectively, and the growth time was about 30 minutes. Then the as-prepared CNTs were transferred to a vacuum chamber at a base pressure of  $1.0 \times 10^{-7} \text{ Pa}$  for the FE measurements. A diode configuration with a moveable anode was employed, the as-prepared CNTAs were stuck on a copper cylinder as the cathode, and the distance between the anode and the cathode was 2.362 mm. During the FE measurements, a voltage ranging from 0 - 10 keV was applied to the anode, the emission current density

\*E-mail: gacheng@bnu.edu.cn; Fax: +86-10-62205403

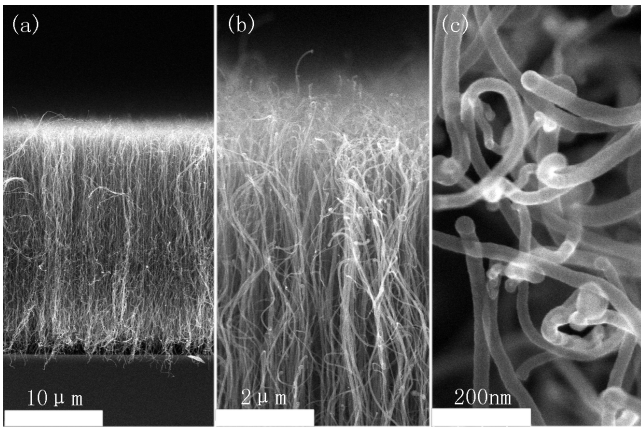


Fig. 1. SEM images of CNTAs: (a) a low-resolution side-view image that shows a panoramic view of the CNTAs, (b) a magnified side-view image near the top of the CNTAs, and (c) a top-view image of the CNTAs.

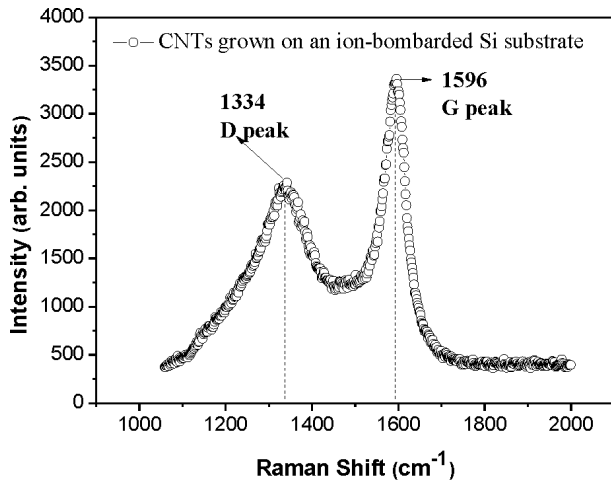


Fig. 2. Raman shift spectrum of the as-grown CNTAs.

versus time (stability) measurements were automatically controlled by using a computer with our own designed programs, and the temperature in all the tests was about 288 K (cooled by water). Scanning electron microscopy (SEM, JSM-4800) and Raman spectroscopy were utilized to determine the structures of the as-prepared CNTAs.

The SEM images of the as-grown CNTAs are shown in Fig. 1. From the panoramic view of CNTAs, as shown in Fig. 1(a), the CNTAs are found to be well aligned on the Si substrate and to be about  $24\ \mu\text{m}$  in length. Figure 1(b) shows a side view of near the top of the CNTAs and clearly reveals that the density of CNTs, especially in near the top, is much lower than that in some other reports [11,12]; *i.e.*, the CNTAs are not densely packed. We attribute this low density of CNTs to the influence of the iron film, which is pre-bombarded on the Si substrate; the additional introduction of iron will blend in the catalyzed iron and increase the thickness of the catalyst. The incorporation of the catalyst can, to a certain

Table 1. Experimental data from the stability measurements.

Emission current density (mA/cm <sup>2</sup> )	Dropping rate (%)	$S_d/J_{\text{mean}}$ (%)
2.99	53.96	6.83
6.43	1.23	0.73
11.02	-3.75	1.27
26.91	-18.61	5.01
21.86	0.66	0.42

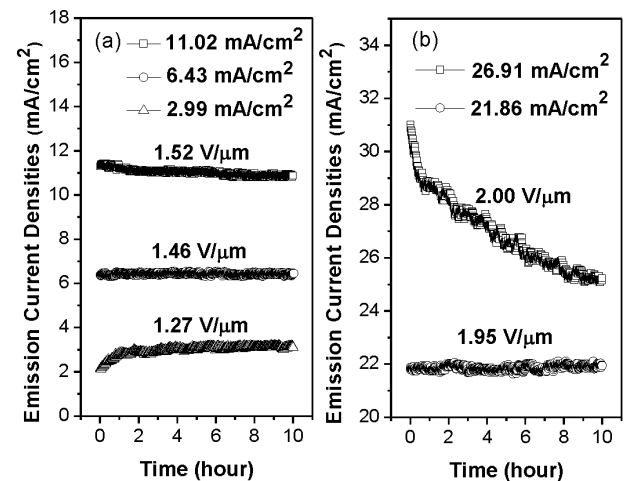


Fig. 3. Stability measurements of CNTAs: (a) stability behaviors of CNTAs under different applied fields, and (b) Stability behaviors of CNTAs under high applied fields.

degree, increase the diameter and reduce the density of the catalyzed grains, which directly determine the diameter and the density of CNTs. Figure 1(c) shows a magnified top-view SEM image, and the diameters of CNTs are found to be about 30 - 50 nm. The catalyst is encapsulated in the tip of the CNT. From all three images, it's not hard to see that the tops of the CNTs are not vertically aligned due to the lower action of the van der Waals force, so some CNTs are buried by others and some extrude from others, which makes the surface of the CNTs uneven rather than smooth.

In order to further understand the microstructure of the CNTs, we employed Raman spectroscopy. Figure 2 shows the Raman shift of the as-grown CNTAs; the evidently broadened D peak ( $1334\ \text{cm}^{-1}$ ), which reflects the amount of disordered carbon in the CNTs [13], demonstrates that the existence of defects appears inevitable in CNTs even without the introduction of any post treatment.

The stability behavior of field electron emission for the CNTAs was studied. Prior to the FE measurements, an aging process [14] was carried out when the emission current density was above  $10\ \text{mA/cm}^2$  for 5 hours to weaken the influence of adsorbates [15]. Figure 3 shows the stability curves of CNTAs under different applied

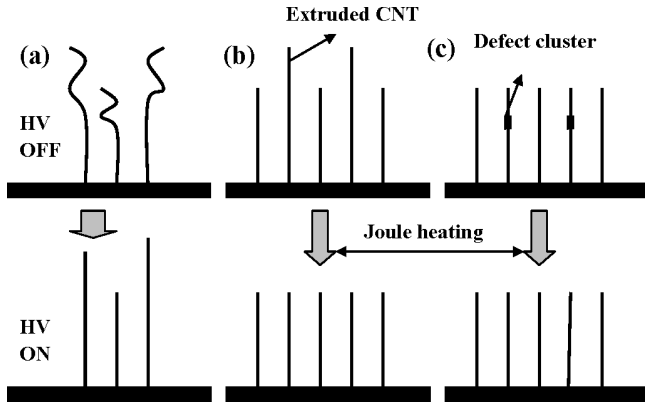


Fig. 4. Schematic illustrations of the mechanisms that bring diversification to the emission current density during stability measurements: (a) curved CNTs straightened by electrostatic force which will directly increase the number of emission sites, (b) extruded CNT burn-off, and (c) defect-rich CNT annealing for the existence of Joule heating which will deteriorate the field electron emission.

fields. The experimental results are presented in Table 1, and two parameters, *i.e.*, the dropping rate and  $S_d/J_{\text{mean}}$ , are introduced to make the discussion convenient. The dropping rate, which is defined as  $(J_{\text{last}} - J_{\text{beginning}})/J_{\text{mean}}$ , is a parameter that directly reflects the degradation of the emission current density while  $S_d/J_{\text{mean}}$ , which is the ratio of the standard deviation to the mean of the emission current densities, to a certain degree, reveals the fluctuation of the emission current densities during field electron emission. From Table 1, the values of the dropping rate and “ $S_d/J_{\text{mean}}$ ” are found to vary with the current density or the applied field. Combining this with Fig. 3(a), we find that three curves are quite different. At an applied field of  $1.27 \text{ V}/\mu\text{m}$ , at which the mean value of the emission current densities is about  $2.99 \text{ mA}/\text{cm}^2$ , the emission current density increases gradually with increasing measuring time for the first two hours; then, the emission current density reaches an equilibrium state in the last 8 hours. The increase in the emission current density is about 53.96% during the 10-hour measurement. At an applied field of  $1.46 \text{ V}/\mu\text{m}$ , at which the mean value of the emission current densities is about  $6.43 \text{ mA}/\text{cm}^2$ , the change in the emission current density is about 1.23%, which is relatively small. However, with a further increase in the applied field to  $1.52 \text{ V}/\mu\text{m}$ , at which the mean value of the emission current densities is about  $11.02 \text{ mA}/\text{cm}^2$ , a 3.75% degradation of the emission current density is obtained. In order to illustrate these differences in emission current densities under different applied fields, we introduce three mechanisms: curved CNT straightening, extruded CNT burn-off, and defect-rich CNT annealing.

Factors, which will influence the field electron emission, are complex and change with time, and it's hard for us to clarify or quantitatively determine each of them. However, a qualitative illustration may be beneficial for

us to find the dominating factors in different cases. Figure 4 shows schematic illustrations of the mechanisms that cause difference in the emission current density during stability measurements. As we know, electrons will agglomerate at the tips of the CNTs during field electron emission, and an electrostatic force will be generated between these negative charges at the tips of the CNTs and the positive charges on the surface of anode. In Fig. 4(a), the curved CNT is straightened by the electrostatic force when the applied field is on, which will directly increase the number of emission sites and improve the FE characteristics. The deformation of the CNT is recoverable, the existence of this electrostatic force has been proven by a previous research [16], and the duration of the straightening process decreases with increasing applied field. Figures 4(b) and (c) reveal the influence of Joule heating, which arises from electrons transiting through CNTs, on the stability behaviors [17]. The uneven surfaces of CNTAs, as shown in Fig. 1, provide a possibility for some CNTs to extrude from others when the applied field is on, and those CNTs will show a relatively large emission current due to a lower field screening effect and a larger aspect ratio [18,19], which means that these extruded CNTs have a greater chance of being burned off due to the Joule heating effect than the lower ones surrounding them. Figure 4(b) is a schematic illustration of this process. Combined with the Raman analysis, as shown in Fig. 2, we find that CNTs have a great many defects, and as is known to all, defects will greatly reduce the CNT's local conductance with an exponential decay [20]. It's not hard to imagine that the resistance will be greatly increased in a certain part of the CNT if there is an agglomeration of defects, in other words, a defect cluster. Therefore, the Joule heating generated in these parts will be larger than that generated in the other parts of CNT, which means that the defects in these parts are more likely to be annealed by the Joule heating and that the reduction in the number of defects, especially vacancy-related defects, will largely deteriorate the FE characteristics [13]. Figure 4(c) just shows a schematic illustration of this condition. Both the extruded CNT burn off and the defect-rich CNT annealing will exert bad effects on the FE characteristics.

According to Fig. 3(a) and Table 1, the stability behavior of the emission current density is mainly controlled by the curved CNT straightening effect when the applied field is low, and this process will terminate with the emergence of a stable emission current density. Because an aging process of CNTAs at above  $10 \text{ mA}/\text{cm}^2$  for 5 hours has been carried out, the influence of the Joule heating effect on CNT burn-off will be negligible at low applied fields. Through a comparison with the other two curves (Fig. 3(a)), the lowest dropping rate and  $S_d/J_{\text{mean}}$  were observed at an applied field of  $1.46 \text{ V}/\mu\text{m}$ . In this case, the extruded CNT burn-off effect should be taken into consideration. As time goes by, more and more new emission sites will emerge due to more curved CNTs being straightened by the elec-

trostatic force, which means that new extruded CNTs will be obtained, and these extruded ones will be more likely to be burned off by the Joule heating effect, which will degrade the emission current density during stability measurements. Therefore, the stability behavior in the middle curve is a combined effect of curved CNT straightening and extruded CNT burn-off. For emission at a high current density, as shown in Fig. 3(a), the emission current density decreases 3.75% in a 10-hour measurement. Under this condition, defect-rich CNT annealing can never be negligible. When a relatively large emission current transits a CNT, the temperature generated in these defect-rich parts due to the existence of Joule heating will be high enough for annealing. Simultaneously, Joule-heating induced CNT burn-off is carried out in a full swing for the emergence of new extruded CNTs. Both the Joule-heating induced CNT burn-off and the defect-rich CNT annealing will continue until the emission current density comes to an equilibrium state, and the duration of this state largely depends on the applied electric field. Hence, for the curve with a high emission current, the Joule-heating induced extruded CNT burn-off and the defect-rich CNT annealing effect are the main causes for the deterioration of the stability behavior.

Figure 3(b) shows the stability behaviors of field electron emission of CNTs at current densities above 20 mA/cm<sup>2</sup>. When a relatively high electric field (2.00 V/ $\mu$ m) is applied, the emission current density decreases from 31.01 mA/cm<sup>2</sup> at the beginning to 25.24 mA/cm<sup>2</sup> at the end, and the dropping rate of the emission current density is about 18.61% during a 10-hour measurement. In this test, light emission is observed at the surface of CNTAs, which indicates that a high emission current is transiting through the CNTs and that heat is generated in them or, at least, in their tips. After the electron emission at an applied field of 2.00 V/ $\mu$ m for 10 hours, another stability measurement was carried out at an applied field of 1.95 V/ $\mu$ m, which is shown in Fig. 3(b). The mean emission current density at an applied field of 1.95 V/ $\mu$ m was about 21.86 mA/cm<sup>2</sup>, and the dropping rate of the current density and the  $S_d/J_{\text{mean}}$  value were 0.66% and 0.42%, respectively, which are much less than the values obtained at the applied field of 2.00 V/ $\mu$ m. At the same time, the light emission induced by Joule heating in the CNTs disappears during the measurement at an applied field of 1.95 V/ $\mu$ m. As is known, the intensity of light emission from CNTs depends on the emission current density, and an ultra-high current density transiting through CNTs will induce Joule heating in CNTs and cause CNTs to emit light. After an aging process at a higher emission current density, the extruded CNTs are burned off and the defect-rich CNTs are annealed, so uniform, smooth and lower-defect CNT arrays are formed. Furthermore, after this treatment, the emission current tends to transit symmetrically through each CNT, which will weaken the Joule heating effect. Based on this aging process, a stability behavior without evident degradation was obtained at a current density of 21.86 mA/cm<sup>2</sup> for

10 hours. The experimental results show that the stability behaviors of field electron emission of CNTAs can be improved greatly by aging at a higher emission current density, which is good considering applications with high emission current densities.

### III. CONCLUSION

The stability behaviors of CNTAs have been studied, and a detailed analysis of the causes that bring about diversifications in the emission current density is discussed. There are three mechanisms to illustrate these diversifications: *i.e.*, curved CNT straightening, extruded CNT burn-off, and defect-rich CNT annealing. Curved CNTs straightened by electrostatic forces will increase the number of emission sites and enhance the FE characteristics, and this effect plays a dominant role at low emission current density. With increasing emission current density, Joule-heating induced extruded CNT burn-off and defect-rich CNT annealing play more important roles than curved CNTs straightening, and an inevitable degradation in the emission current density is introduced at a high emission current density. A stability behaviour, without evident degradation at 21.86 mA/cm<sup>2</sup> in 10 hours, is obtained after an aging process at a higher emission current density. Based on these results, an aging process at a higher emission current density can strongly improve the stability behavior of the field electron emission of CNTs and is an effective way to realize long-term stable field electron emission.

### ACKNOWLEDGMENTS

This work is supported by the National Basic Research Program of China (No. 2010CB832905) and partially by the Key Scientific and Technological Project of the Ministry of Education of China (No. 108124).

### REFERENCES

- [1] S. Iijima, *Nature* **354**, 46 (1991).
- [2] R. H. Baughman, A. A. Zakhidov and W. A. de Heer, *Science* **297**, 787 (2002).
- [3] R. T. Zheng, G. A. Cheng, Y. B. Peng, Y. Zhao, H. P. Liu and C. L. Liang, *Sci. China, Ser. E Eng. Mater. Sci.* **47**, 616 (2004).
- [4] H. P. Liu, G. A. Cheng, R. T. Zheng, Y. Zhao and C. L. Liang, *J. Mol. Catal. A: Chem.* **247**, 52 (2006).
- [5] H. P. Liu, G. A. Cheng, R. T. Zheng, Y. Zhao and C. L. Liang, *Surf. Coat. Technol.* **202**, 3157 (2008).
- [6] S. F. Lee, Y. P. Chang and L. Y. Lee, *New Carbon Mater.* **23**, 104 (2008).
- [7] C. K. Dong and M. C. Gupta, *Appl. Phys. Lett.* **83**, 159 (2003).

- [8] R. B. Rakhi, K. Sethupathi and S. Ramaprabhu, Appl. Surf. Sci. **254**, 6770 (2008).
- [9] B. Q. Zeng, G. Y. Xiong, S. Chen, W. Z. Wang, D. Z. Wang and Z. F. Ren, Appl. Phys. Lett. **89**, 223119 (2006).
- [10] G. H. Chen, D. H. Shin, S. Kim, S. Roth and C. J. Lee, Nanotechnology **21**, 015704 (2010).
- [11] B. J. Hinds, N. Chopra, T. Rantell, R. Andrews, V. Gavalas and L. G. Bachas, Science **303**, 62 (2004).
- [12] B. D. Sosnowchik and L. W. Lin, Appl. Phys. Lett. **89**, 193112 (2006).
- [13] T. Tanabe, Phys. Scr. T **64**, 7 (1996).
- [14] W. H. Liu, X. Li and C. C. Zhu, Ultramicroscopy **107**, 833 (2007).
- [15] C. Li, G. J. Fang, X. X. Yang, N. S. Liu, Y. P. Liu and X. Z. Zhao, J. Phys. D: Appl. Phys. **41**, 195401 (2008).
- [16] W. Wei, K. L. Jiang, Y. Wei, M. Liu, H. T. Yang, L. N. Zhang, Q. Q. Li, L. Liu and S. S. Fan, Nanotechnology **17**, 1994 (2006).
- [17] K. A. Dean, T. P. Burgin and B. R. Chalamal, Appl. Phys. Lett. **79**, 1873 (2001).
- [18] S. J. Kyung, J. B. Park, B. J. Park, J. H. Lee and G. Y. Yeom, Carbon **46**, 1316 (2008).
- [19] J. S. Suh, K. S. Jeong and J. S. Lee, Appl. Phys. Lett. **80**, 2392 (2002).
- [20] G. Wei, Appl. Phys. Lett. **89**, 143111 (2006).